Materials and Design 191 (2020) 108599

Contents lists available at ScienceDirect

Materials and Design

journal homepage: www.elsevier.com/locate/matdes

Effects of impactor shape on the deformation and energy absorption of closed cell aluminium foams under low velocity impact

M.A. Islam [a,c,*], M.A. Kader [b], P.J. Hazell [a], J.P. Escobedo [a], A.D. Brown [a], M. Saadatfar [b]

[a] School of Engineering and Information Technology, The University of New South Wales, Canberra, ACT 2610, Australia
[b] Department of Applied Mathematics, Research School of Physics, The Australian National University, Canberra, ACT 2601, Australia
[c] Department of Mechanical Engineering, Khulna University of Engineering and Technology, Khulna 9203, Bangladesh

HIGHLIGHTS

- Dynamic indentation response of closed-cell aluminium foam depends on indenter's nose shape.
- Specific energy absorption increases with the increase of impact velocity.
- Nose shape of impactor influences the deformation behaviour and energy absorption in closed-cell foams.
- Deformation in dynamic indentation initiates just underneath the indenter and propagates with the indenter's movement.

GRAPHICAL ABSTRACT

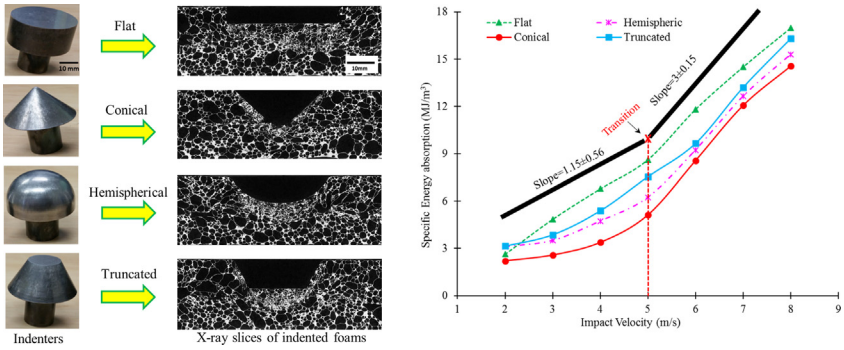

ARTICLE INFO

Article history:
Received 23 October 2019
Received in revised form 7 February 2020
Accepted 24 February 2020
Available online 24 February 2020

Keywords:
Indentation
Closed-cell aluminium foam
Energy absorption
Collapse mechanisms
Low-velocity impact

ABSTRACT

The low-velocity impact response of closed-cell aluminium foams using various shaped indenters has been investigated. Impact tests were conducted using an instrumented drop-tower with flat, hemispherical, conical and truncated-conical indenter at impact energies ranging from 46.8 J to 105 J. The effects of variation of indenter shape and impact velocity on mechanical properties and deformation mechanisms of foam have been explicitly investigated. The results show that the mechanical response of closed-cell aluminium foams under low-velocity projectile impact significantly depends on the indenters' nose shape and initial impact energy. The deformation mechanisms of foam for different shaped indenters have been elucidated using reconstructed X-ray micro-computed tomography (XCT) images of the indented specimens. A good correlation between the indenter shape and deformation mechanisms has been observed. The structure-property relations of foams during dynamic indentation have also been explored by analysing the XCT images of the indented specimens. The parameters that influence the energy absorption capacity of the material are also presented.

1. Introduction

Closed-cell aluminium foams have excellent properties such as low density as well as a relatively high stiffness and high-energy absorption during impact loading. These properties make them attractive materials for a wide range of applications. Their use

* Corresponding author at: School of Engineering and Information Technology, The University of New South Wales, Canberra, ACT 2610, Australia.
E-mail address: md.islam@me.kuet.ac.bd (M.A. Islam).

https://doi.org/10.1016/j.matdes.2020.108599

extends to the automotive, aerospace, military and defence industries [1,2]. These materials are especially important for application within the packaging industry where a protected product may be susceptible to point-load or blunt impact, from which it needs protection during transit. Application as a sacrificial cladding is also possible as they deform to very large plastic strains [3]. Several studies have examined the strength variation of aluminium foams with increasing strain rates [4–7]. Numerous studies have examined the mechanical response of these materials during quasi-static or constant impact velocity loading [8–14] and noted that closed-cell aluminium foams possess significant potential to be used in different load bearing and energy absorbing applications. A number of research groups manufactured syntactic foams and studied their compressive behaviour during quasi-static and dynamic loadings [15–20]. They reported that the topology of syntactic foams is comparatively easy to control, and the foams show good mechanical performance during loadings. Although the manufacturing methods of these syntactic foams have good controllability over the pore shape, pore size and porosity distribution, the hollow fillers highly likely behave differently from the metal matrix and possibly affect the mechanical performance. Kader et al. [21] studied the deformation mechanisms of closed-cell aluminium foams using XCT based reconstructed samples and finite element (FE) simulations during quasi-static compressive loading. They concluded that the mechanical properties of closed-cell foam structures significantly depended on their geometry and cell collapse mechanisms. The dynamic deformation mechanisms and mechanical behaviour of aluminium foams have also been studied in previous works [11,22], and observed layer-wise deformation in low and medium velocity impacts. Sun et al. [23] investigated the strain-rate effect on the compressive behaviour of closed-cell aluminium foam using X-ray CT based FE modelling and reported that the rate dependency of cell-wall material dominates the macro strain-rate effect on the compressive strength, whereas the micro strain-rate has very small effect for Alporas foam. However, spontaneous or non-constant velocity impact and localised penetration at low velocity are the most common phenomena these materials are likely to experience in their working environments [24–27], and there has been relatively little work done on these materials in this regime [28,29]. Consequently, little to no information is available on the structural and morphological changes in dynamically indented foam materials. Olurin et al. [26] investigated the indentation response of metallic foams with different indenter geometries. Flores-Johnson and Li [30] also studied the impactor nose shape effects on polymeric foams and noted that the penetration load depends on the shape of the indenter and density of the foams. A few research groups studied the effect of indenter shape during indentation in foam cored sandwich panels [31,32] and explained the damage and collapse mechanisms observing outer surface or cross section of the indented samples. However, the single surface observations of the indented samples will not be able to provide the actual deformation/collapse mechanisms and their effects on the mechanical response. Thus, it is necessary to investigate the complete volume of the indented samples using XCT to explore the actual scenario of penetration during indenting with different shapes indenters.

In this work, we have conducted indentation experiments on closed-cell aluminium foam using four different shaped indenters. The effects of indenter shape on the collapse mechanisms and mechanical properties have been evaluated. The effect of velocity variation and indenter shape on energy absorption capacity of foam has been also been investigated. The specimens have been imaged after indentation using the XCT facility of Australian National University (ANU). The detail collapse mechanisms and their consequences on mechanical properties have also been explored through observing the XCT based images.

2. Materials and methods

2.1. Materials

In this study, CYMAT™ stabilized aluminium foams (SAFs) with density of 0.51 g/cc were used which was manufactured by the direct foaming technique [33]. The bulk alloy [34] is melted and then stabilized particles consisting of ceramic compounds (SiC/Al_2O_3) are added to the molten materials during processing, which is subsequently poured into a foaming box. Bubbles are created by injecting gas (air) in a controlled fashion through a rotating impeller resulting in a foam structure. The cell size is controlled by varying the operating conditions, such as gas pressure and temperature. The base material consisted of 8–10% Silica, 0.5% magnesium, <1% iron and copper [9]. Two samples of 40 mm × 40 mm × 23 mm dimensions have been prepared for each of the compression experiments. In addition, two samples of 120 mm × 120 mm × 23 mm dimensions have been prepared for each of the indentation experiments. A typical macroscopic and microscopic view of a foam sample is shown in Fig. 1. It is observed that the cell walls thickness and cell size distribution is significantly heterogeneous throughout the sample. As seen from the representative foam structure in Fig. 1(c) and (d), the cell sizes distribution for this aluminium foam are heterogeneous and have an overall irregular morphology.

The morphological properties of the foams are measured and presented in Table 1. These properties have been measured considering three small representative areas and each area contained ~50 cells.

2.2. Mechanical tests

2.2.1. Quasi-static compression

Quasi-static compaction and indentation tests were carried out using a Shimadzu Universal Testing Machine by inserting each indenter (four different shapes) into a crosshead affixed with a 50 kN capacity load cell. The sample was placed at the middle of the bottom platen. The contact surfaces between the sample and platens have been lubricated to reduce the effect of friction. The compressive load was applied under a constant crosshead velocity of 1.4 mm/s, which resulted in a nominal strain rate of $10^{-3}\,s^{-1}$. Two samples (40 mm × 40 mm × 23 mm) for each of the test condition have been tested to confirm the repeatability of results and the average result has been reported. The force data were directly recorded by the load cell and the displacement of the top platen was also recorded by the data accusation system of the machine. Then the stress and strain are calculated from the following equations: Stress, $\sigma = {}^{F}/_{A}$ where F is recoded force data and A is the area of the specimen before deformation, and strain $\varepsilon = {}^{d}/_{L}$ where d is the recorded displacement and L is the height of the specimen before deformation.

2.2.2. Drop-weight impact experiments

The dynamic compression and indentation tests were carried out at impact velocities ranging from 2 to 8 m/s with an instrumented drop tower (CEAST 9350) equipped with a 90 kN force sensor, shown in Fig. 2. The samples with 90 mm × 90 mm × 23 mm dimensions were used for the drop-tower indentation tests. Two samples were tested for each of the test condition to confirm the repeatability of results and the average result has been reported. The falling mass was kept at a constant 5.85 kg. Samples were clamped to a flat rigid plate to ensure rigid boundary conditions throughout the tests. Four different shaped indenters have been used for the dynamic tests, and their geometric profiles are presented in Fig. 3. The drop heights have been varied to get the desired impact velocities. We achieved 4, 5 and 6 m/s impactor velocities for the drop heights 0.81 m, 1.27 m and 1.83 m respectively.

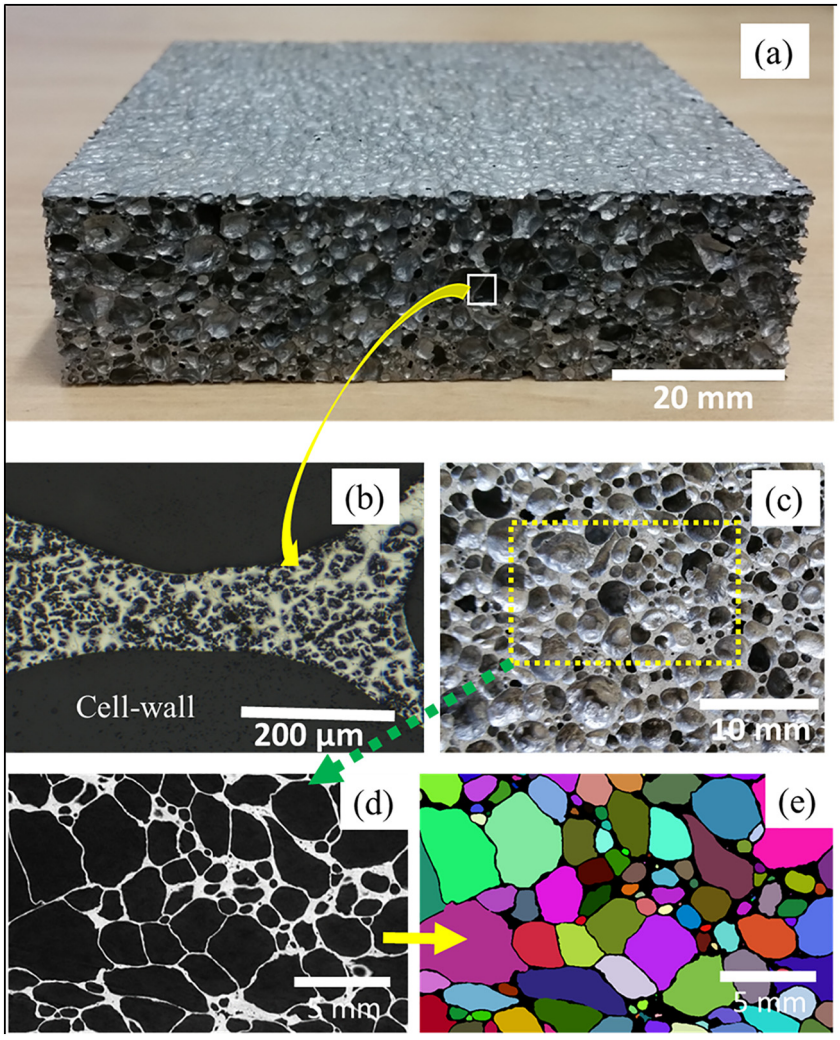

Fig. 1. The macro-structural and microstructural characteristics of closed cell aluminium foam: (a) foam sample, (b) cell-wall cross-section (Optical Microscopy), (c) representative foam structure, (d) XCT slice of a foam sample, and (e) individual pore (cavity) identification based on the XCT data. Note that the colours have no significant meaning and they are intended to show individual pores in the foam sample.

2.2.3. X-ray CT procedure

The test specimens were imaged via XCT (voxel resolution 44 μm) after deformation. A flat panel detector (pixel size 0.14 μm) and micro focus X-ray source (acceleration voltage 100 kV and current 100 μA) both supplied by Hamamatsu (Japan), were used for imaging. The foam specimen was placed on a motor controlled rotating stage, and radioscopic projections were taken after each degree of rotation. In total, around 10,000 projections were obtained for a complete rotation of the foam. The exposition time was 4 s and two images per projection were averaged to reduce the noise. The total imaging time was approximately 22 h for each sample. The raw tomography images were processed in Medial Axis and Network Generation (MANGO) software tool to acquire suitable images of the indentation. Anisotropy Diffusion (AD) and Unsharp Musk (UM) filters available in MANGO have been used to clean the raw tomographic images.

3. Results and discussions

3.1. Mechanical responses

The stress-strain response during quasi-static and drop-weight compression tests of the closed-cell foam is shown in Fig. 4. It is observed that the impact responses are significantly higher than the quasi-static responses which agree with the previous works on Cymat foams [35,36]. The rate dependency of the base materials, micro- and macro-inertias and entrapped air are the main possible reasons behind the stress enhancement during impact loadings [37]. The stress-strain responses from drop weight impact loading display oscillations, which possibly because of repetitive cycles of plastic collapse in the weak bands of the specimen until the entire foam becomes densified. Similar oscillations were also found under dynamic loadings in [30,35,38,39] for these materials.

Table 1
The morphological properties of CYMAT closed cell foams.

Density (g/cc)	Relative density (%)	Average cell size (mm)	Cell-wall thickness (mm)	Alloy composition [9]
0.51	18.88%	1.75 ± 1.13	0.21 ± 0.09	Al + Si(10%) + Cu(<1%) + Mg(<0.5) + Fe (<1%) + Ti (0.2%)

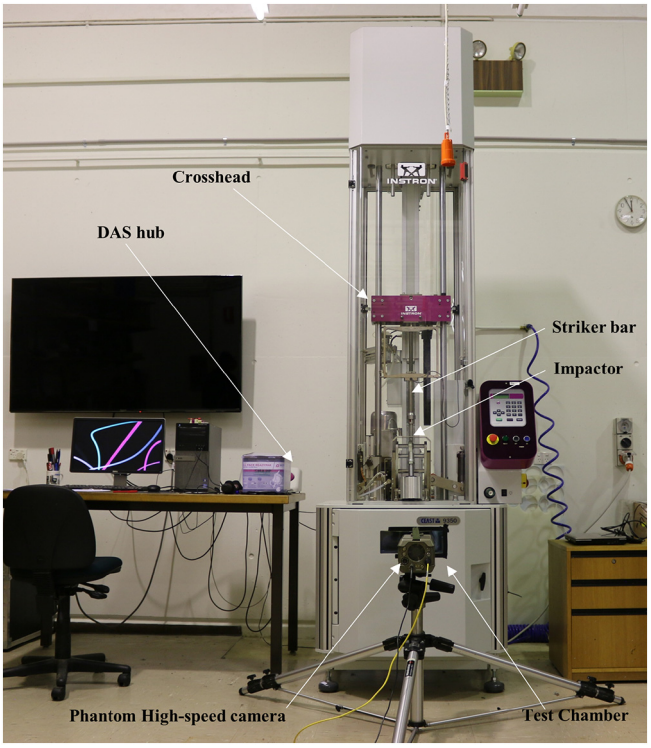

Fig. 2. Photograph of the experimental setup for the drop impact tests.

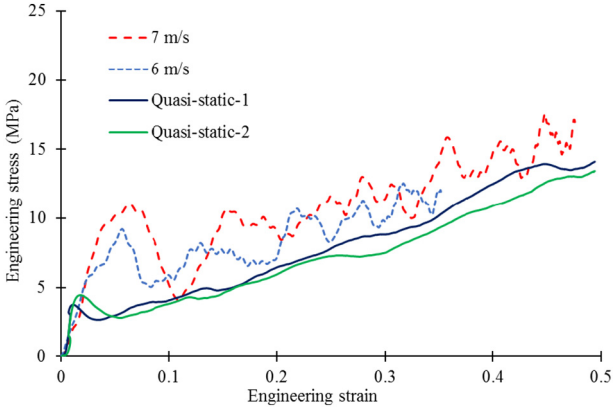

Fig. 4. Stress-strain curves in quasi-static (QS) and drop weight impact tests.

Fig. 5 shows the force-displacement response of the foam for four different indenters under quasi-static (Fig. 5(a)) and drop weight impact (Fig. 5(b)) loadings. It is observed that the force-displacement response for various shaped indenters show almost similar overall behaviour during quasi-static and dynamic indentations except the oscillation arising during the dynamic indentations. In the case of the flat indenter, the dynamic force-displacement response is nearly similar to the quasi-static response within elastic region, and then the plastic collapse continued with the densification of foam underneath the indenter. The plastic load steadily increased due to crush propagation resulted in a densified zone that created further resistance to indentation. Later in time, the forces that induced plastic deformation were increased due to tear, stretching and friction in the material. This occurred for all the indenters. Notably, the force-displacement curve of the flat indenter exhibited a lower elastic loading slope compared to the elastic slopes of all other indenter shapes. In the case of the conical indenter, the force increased gradually with the depth of indentation due to the increase of the indenters' cross-section. The crushed zone in the surrounding area and friction in the inclined indented specimen increased during the impact and resulted in the steady increase of load.

The truncated-conical indenter shows a more interesting response. This was similar to that of the flat indenter in the beginning and a combined flat and conical indenter for the rest of the curve. It was assumed that a continuous crushing of foam underneath the indenter as well as tearing of the cell walls and frictional work occurred during the entire penetration phase.

The response of dynamic indentation in the foam samples for all four indenters are further evaluated for the variation of impact velocity and presented in Fig. 6(a–d). It was observed that the load increased with increasing impact velocity for most of the impactor shapes. This supports the view that these materials exhibit strain-rate sensitivity and agrees with the findings of previous works [35]. Moreover, the indentation depth increases with increasing impact velocity for all of the indenter tips. The impact energy also increases with increasing impact velocity and consequently the foam sample experienced additional depth of penetration at higher impact velocities.

Fig. 7 shows the impact velocity attenuation and energy absorption during the impacts. It is seen that the velocity attenuation with the flat and hemispheric indenter is quicker than the truncated and conical indenters. The velocity attenuation and energy absorption rate are strongly related with the deformation and collapse mechanisms of foam during impact. The possible reasons of variation of velocity

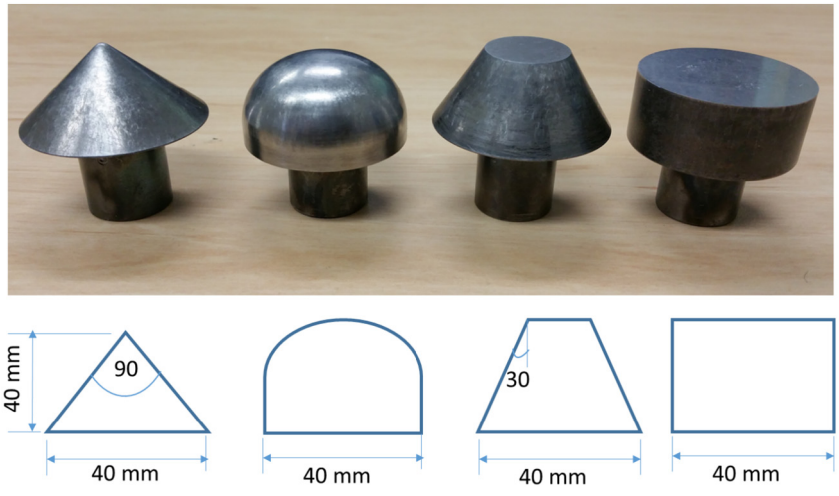

Fig. 3. Indenters' profiles: conical, hemispheric, truncated and flat (from left to right).

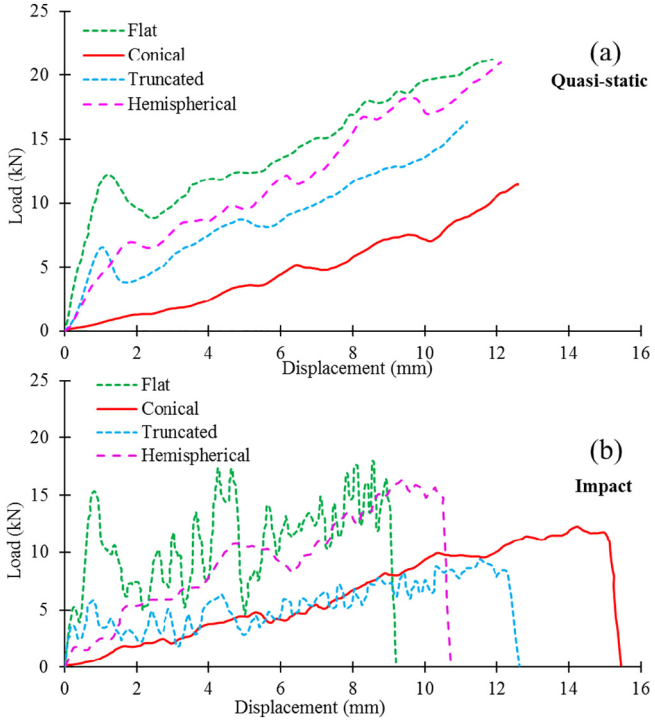

Fig. 5. Force vs indentation displacement curves: (a) quasi-static indentation tests, and (b) drop-tower indentation tests at 6 m/s.

attenuation and energy absorption rate will be explored with the aid of XCT images in Section 3.2.

The specific energy absorption for different indenters' tips has been plotted in Fig. 8. To calculate the specific energy, first, the total energy absorbed by the foams has been calculated from the force-displacement curve for each indenter. Secondly, the indented volume for each indenter was calculated from the 3D reconstructed X-ray μ-CT data. Therefore, the specific energy was calculated from total energy absorbed by the foam divided by the indented volume of the foams. It was observed that the energy absorption per-unit-deformed volume (specific energy absorption, MJ/m^3) increases with the increase of impact velocity for all of the studied impactor shapes. The increase of specific energy absorption with the increase of impact velocity is evidence of the strain-rate sensitivity of closed-cell aluminium foams as reported in other dynamic studies [22,35,40]. It is seen that specific energy absorption in the flat indenter was higher than all the other indenters. The reasons of higher energy absorption by the flat indenter are, likely to be due to: i) large crushed zone of compressed material underneath the flat surface, and ii) extra work required to tear its cell walls due to shear, friction and stretching. On the other hand, the indentation with the conically-shaped indenter absorbed comparatively less amount of energy for all of the studied impact velocities. The reason for this was that the foam experienced comparatively less shear failure and cell-wall tearing.

It is observed that the specific energy absorption capacity for all of the studied indenters increased gradually up to 4 m/s impact velocity and then sharply increased from 5 m/s impact velocity. To interrogate this behaviour, the slopes of the curves, between 2–4 m/s and 5–8 m/s ranges, have been measured separately for all of the indenters and presented the average values for all of the ranges (thick black lines) in Fig. 8. The average slopes of the range 5–8 m/s is more than double of the slope of 2–4 m/s velocity range. A transition point is noticed at around 5 m/s impact velocity and marked with 'X' letter. This suggests that, the energy absorption capacity of the studied foam would be significantly higher beyond ~5 m/s impact velocity regardless of the indenter tip geometry. The variation of specific energy absorption due to variation of indenter shapes will be further discussed with the aid of XCT images in Section 3.2.

3.2. Deformation analysis

The mechanical responses of foams significantly depend on their geometrical architecture and collapse mechanisms [12,21,41]. Thus, the deformation mechanisms and structure-property relationships of aluminium foam under impact loadings have been elucidated using XCT images of the indented samples. The deformation mechanisms under drop-weight compression loading have been investigated using XCT slices of a sample before and after compaction. The CT slices before and after compression are presented in Fig. 9(a) and (b) respectively. It is observed that the area with relatively large pores and thin cell walls

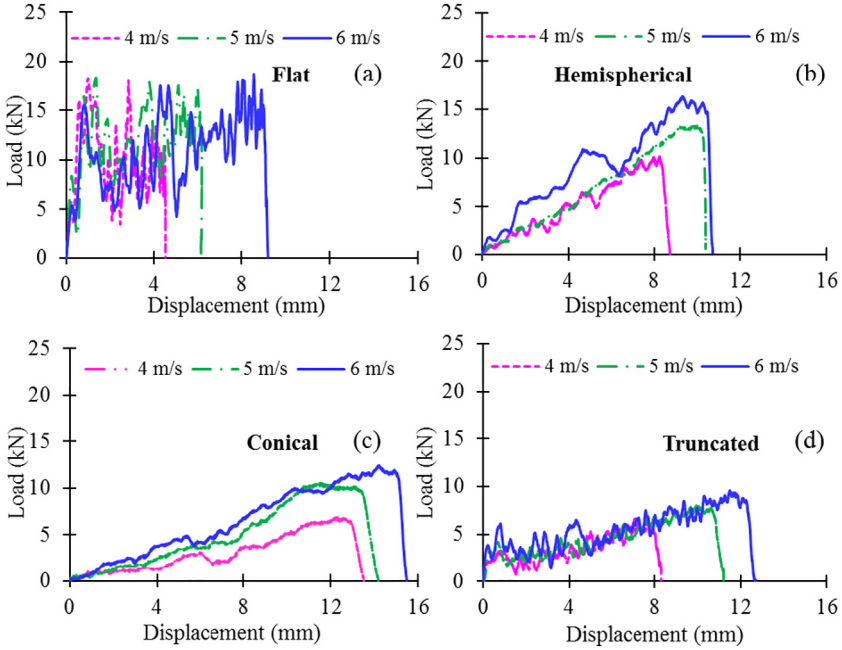

Fig. 6. The effect of impact velocity on the reaction force and indentation depths for four indenters: (a) flat, (b) hemispheric, (c) conical, and (d) truncated indenters.

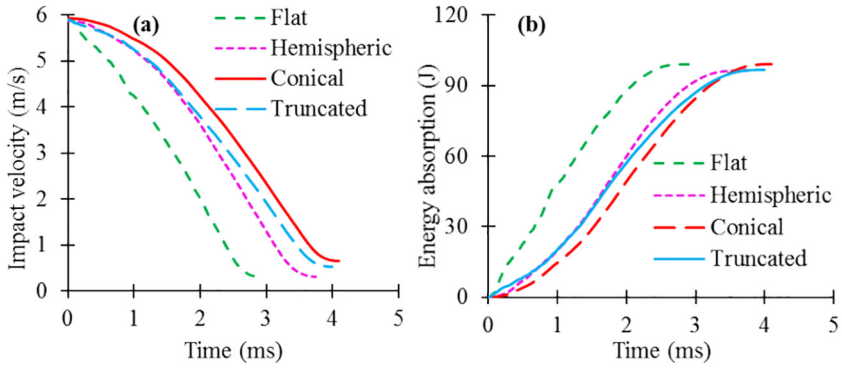

Fig. 7. (a) Velocity attenuation rate and (b) energy absorption rate for four different indenter tips under 6 m/s velocity impact loadings.

preferentially undergoes plastic deformation which agrees with the quasi-static study of Kader et al. on the deformation mechanisms of closed-cell foams [21]. Song et al. [42] also studied the deformation mechanisms of closed-cell aluminium foams and observed similar deformation mechanisms during compressive loadings. That is, the studied foam is significantly heterogeneous and starts deforming from the high porosity region. This region has been demarcated with the yellow dotted lines in Fig. 9.

The deformation mechanisms of foam for four different indenter shapes have also been elucidated by investigating XCT slices of the dynamically indented specimens. These XCT slices with the corresponding indenter tips are presented in Fig. 10. The deformation field of dynamically compacted and indented specimens for the flat impactor can be compared through observing Figs. 9(b) and 10(a). It is observed that the cell collapse started just underneath the impactors' surface during the indentation with flat indenter. Notably, the impact force has been completely absorbed by the collapsed cells just underneath the indenter. On the other hand, the deformation found mainly in the middle zone (relatively high porosity zone) of the sample for the compression tests.

Fig. 10 shows that the deformed cell-walls moved towards the nearby pore spaces and subsequently curled depending on the shape of voids for all of the studied indenters. The XCT slices in Figs. 9 (b) and 10(a–d) also show that the top wall of pores moves towards the voids by forming hinges at weaker positions. The deformation zone shows that the cell walls undergo several modes of deformation such as bending, buckling, tearing and fracture. In general, for dynamic

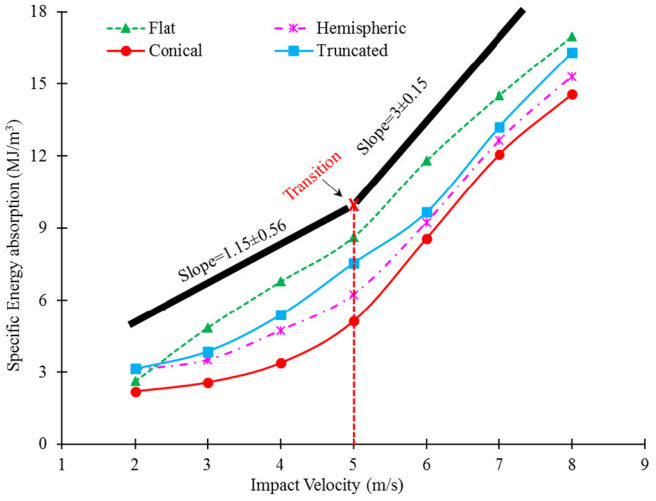

Fig. 8. Variation of specific energy absorption of closed-cell aluminium foam with variation of impact velocities under dynamic indentation with four differently shaped indenters. The thick black lines are the schematic showing the trend of the slope of the experimental curves.

indentation tests it is observed that the maximum amount of pore collapse occurs at just underneath the indenters whereas the cells in the bottom of the sample remain almost undeformed. It is observed from Fig. 10 that the deformation propagates comparatively larger distance from the impactor faces during indentation with a flat indenter whereas small amount of area in the vicinity of the indenter undergoes plastic deformation in case of a conical indenter. The flat indenter also produced maximum amount of shear and tear failures of cell walls during penetration. The foam absorbs comparatively large amount of specific energy during indentation with a flat indenter whereas it absorbs comparatively less specific energy during indentation with a conical indenter for all of the studied impact velocities as observed in Fig. 9. This suggested that the size of deformed area is one of the principal reasons behind the variation of energy absorption during indentation with different indenter tips. The impact with truncated indenter shows comparatively better load plateau during plastic deformation with reasonably higher energy absorption (shown in Figs. 5(b) and 8). The combined shear collapse/tearing at the sides of indenter and plastic deformation of cell walls under the indenter shown in Fig. 10(d) are responsible for an initial higher yield strength and comparatively better load/stress plateau during plastic deformation. The XCT data clearly illustrated the process of deformation that the specimen underwent for different indenter tips. It can be noticed in Fig. 10 that deformation propagated from the impactor surface towards the bottom of the specimen as the indenter moved downward. The movement of adjacent cell-walls in a confined space developed friction which may have had a major contribution to the energy absorption. However, there is no deformation found in the bottom region of the specimens for all the indentation tests. This signified that closed-cell aluminium foams are suitable for impact energy absorption in applications such as used as sacrificial cladding or protective shield from low-velocity projectile impact. They are able to mitigate against potential damage close to the rear of the foam sample if the foam material is sufficiently thick enough.

The XCT data have the potentiality to explain the detail structural changes as a result of indenter impact. Correlating 3D quantification of bulk deformation from XCT data and indenter's tip geometry will be presented in future works.

4. Conclusions

The dynamic compaction and indentation response of CYMAT closed-cell aluminium foams were tested to investigate their cell collapse mechanisms and energy absorption performance. The deformation mechanisms during low-velocity drop impacts were explored using XCT data of the deformed samples. This data and the presented conclusions will be useful to those who are concerned about protecting packages from blunt as well as point-load impacts during transit.

The following specific conclusions can be drawn from the current investigation:

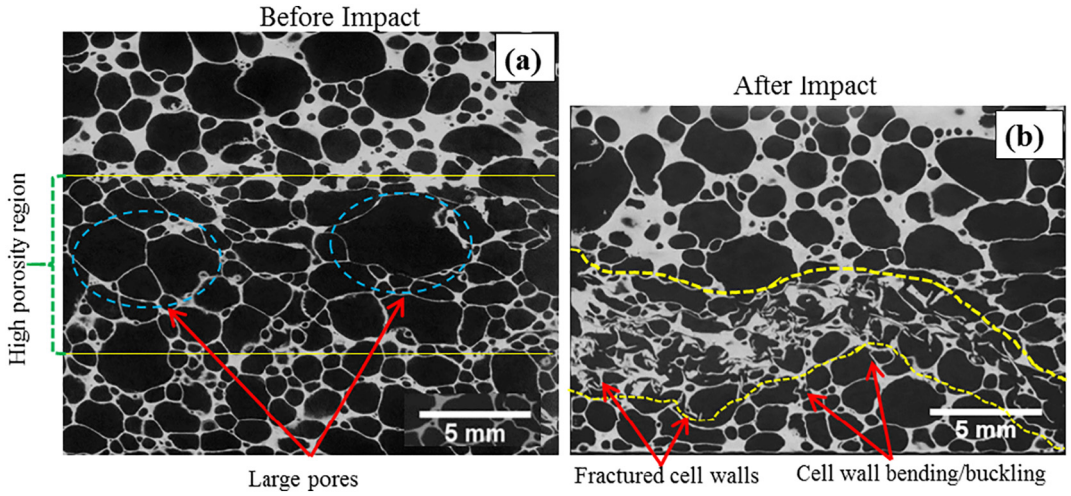

Fig. 9. X-ray density map showing: (a) undeformed specimen, and (b) deformed specimen of the same sample under dynamic compression (impact velocity 6 m/s). The yellow dotted/solid lines indicated the weak band of the foam specimen where the deformation mainly took place.

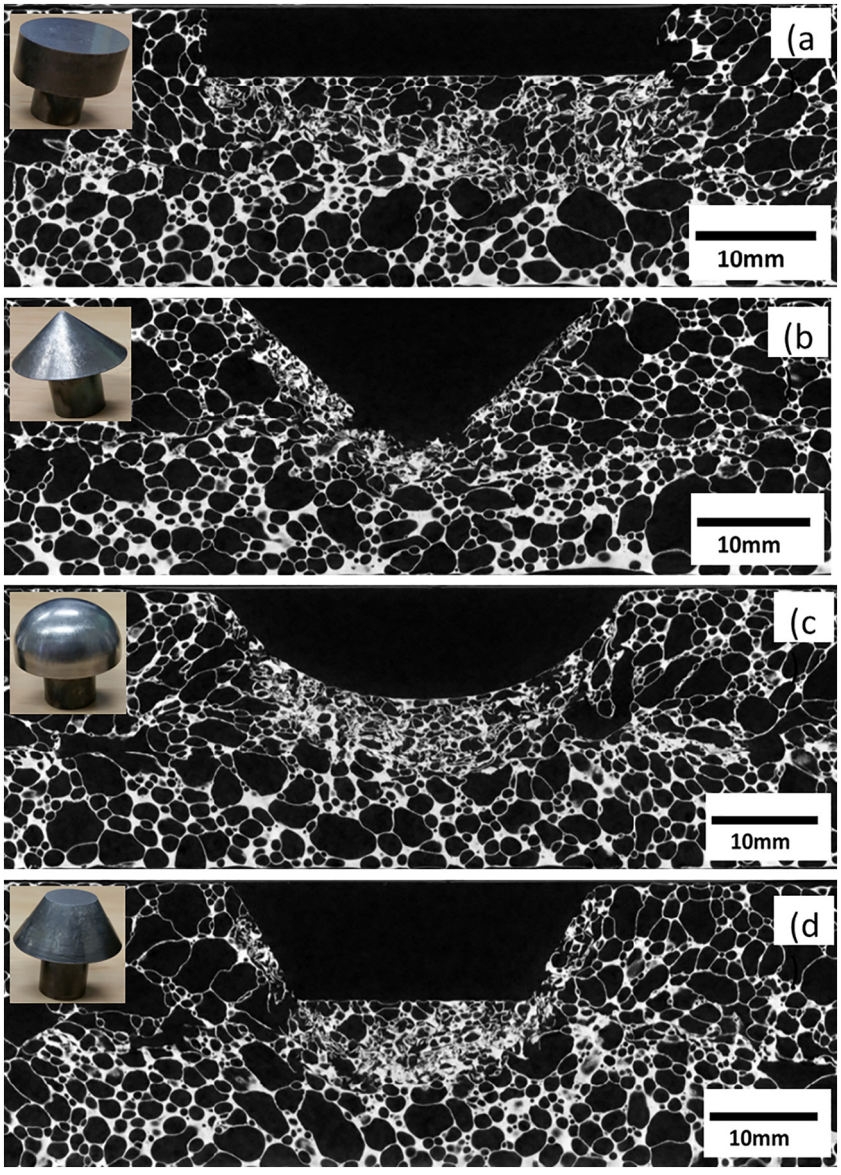

Fig. 10. XCT slices of deformation samples for (a) flat indenter, (b) conical, (c) hemispherical and (d) truncated indenter. The corresponding indenter tips are placed as an inset of this figure. The tests were carried out at an impact velocity of 6 m/s.

- The experimental results show that the response of a closed-cell aluminium foam subjected to a low-velocity impact depends on the indenter's nose shape and the initial impact energy at which the impact occurred.
- The specific energy absorption (energy absorption per-unit-deformed-volume) increases with increasing impact velocity for all of the studied indenter tips. The energy absorption capacity of this foam significantly increases beyond 5 m/s impact velocity. Also, it is found that the specific energy absorption for the flat indentation was higher than other indentation for the same impact velocity.
- Finally, X-ray tomography of the specimens tested during dynamic compression (drop impact) showed that the cell collapse of the foams initiated in a middle (weak) band of the specimen (see Fig. 9). However, deformation in dynamic indentation initiated just underneath the indenter (see Fig. 10) and propagated with the indenter's movement until the foam resistance completely stopped the indenter.

CRediT authorship contribution statement

M.A. Islam: Conceptualization, Methodology, Investigation, Data curation, Writing - original draft, Writing - review & editing, Formal analysis, Visualization, Validation. **M.A. Kader:** Conceptualization, Formal analysis, Writing - original draft, Writing - review & editing, Visualization, Validation. **P.J. Hazell:** Supervision, Resources, Writing - review & editing. **J.P. Escobedo:** Supervision. **A.D. Brown**: Supervision. **M. Saadatfar:**Supervision, Resources, Writing - review & editing.

Declaration of competing interest

We wish to confirm that there are no known conflicts of interest associated with this publication and there has been no significant financial support for this work that could have influenced its outcome.

Acknowledgements

The authors gratefully acknowledge UNSW Canberra's Defence Related Research program that part-funded this work. M.A. Islam also likes to thank M. Turner, L. Beachin and J. Middleton for their technical support in X-ray image analysis in the Department of Applied Mathematics, The Australian National University, Canberra, Australia.

References

[1] J. Banhart, Manufacture, characterisation and application of cellular metals and metal foams, Prog. Mater. Sci. 46 (2001) 559–632.
[2] P.J. Hazell, Armour: Materials, Theory, and Design, 1st, CRC Press, Boca Raton, FL, USA, 2015.
[3] M. Yahaya, D. Ruan, G. Lu, M. Dargusch, Response of aluminium honeycomb sandwich panels subjected to foam projectile impact–an experimental study, International Journal of Impact Engineering 75 (2015) 100–109.
[4] P.S. Kumar, S. Ramachandra, U. Ramamurty, Effect of displacement-rate on the indentation behavior of an aluminum foam, Mater. Sci. Eng. A 347 (2003) 330–337.
[5] J. Shen, G. Lu, D. Ruan, Compressive behaviour of closed-cell aluminium foams at high strain rates, Compos. Part B 41 (2010) 678–685.
[6] E. Andrews, W. Sanders, L.J. Gibson, Compressive and tensile behaviour of aluminum foams, Mater. Sci. Eng. A 270 (1999) 113–124.
[7] E. Andrews, G. Gioux, P. Onck, L. Gibson, Size effects in ductile cellular solids. Part II: experimental results, Int. J. Mech. Sci. 43 (2001) 701–713.
[8] G. Lu, J. Shen, W. Hou, D. Ruan, L. Ong, Dynamic indentation and penetration of aluminium foams, Int. J. Mech. Sci. 50 (2008) 932–943.
[9] M.A. Islam, M.A. Kader, P.J. Hazell, A.D. Brown, M. Saadatfar, M.Z. Quadir, J.P. Escobedo, Investigation of microstructural and mechanical properties of cell walls of closed-cell aluminium alloy foams, Mater. Sci. Eng. A 666 (2016) 245–256.
[10] M. Islam, J. Escobedo, P. Hazell, G. Appleby-Thomas, M. Quadir, Characterization of closed-cell aluminium foams subjected to compressive loading, Characterization of Minerals, Metals, and Materials 2015, pp. 165–174.
[11] M.A. Kader, M.A. Islam, P.J. Hazell, J.P. Escobedo, M. Saadatfar, A.D. Brown, G.J. Appleby-Thomas, Modelling and characterization of cell collapse in aluminium foams during dynamic loading, International Journal of Impact Engineering 96 (2016) 78–88.
[12] M. Saadatfar, M. Mukherjee, M. Madadi, G.E. Schröder-Turk, F. Garcia-Moreno, F.M. Schaller, S. Hutzler, A.P. Sheppard, J. Banhart, U. Ramamurty, Structure and deformation correlation of closed-cell aluminium foam subject to uniaxial compression, Acta Mater. 60 (2012) 3604–3615.
[13] H. Bart-Smith, A.F. Bastawros, D.R. Mumm, A.G. Evans, D.J. Sypeck, H.N.G. Wadley, Compressive deformation and yielding mechanisms in cellular Al alloys determined using X-ray tomography and surface strain mapping, Acta Mater. 46 (1998) 3583–3592.
[14] A.F. Bastawros, H. Bart-Smith, A.G. Evans, Experimental analysis of deformation mechanisms in a closed-cell aluminum alloy foam, Journal of the Mechanics and Physics of Solids 48 (2000) 301–322.
[15] T. Fiedler, M. Taherishargh, L. Krstulović-Opara, M. Vesenjak, Dynamic compressive loading of expanded perlite/aluminum syntactic foam, Mater. Sci. Eng. A 626 (2015) 296–304.
[16] M. Taherishargh, E. Linul, S. Broxtermann, T. Fiedler, The mechanical properties of expanded perlite-aluminium syntactic foam at elevated temperatures, J. Alloys Compd. 737 (2018) 590–596.
[17] E. Linul, D. Lell, N. Movahedi, C. Codrean, T. Fiedler, Compressive properties of zinc syntactic foams at elevated temperatures, Compos. Part B 167 (2019) 122–134.
[18] T. Fiedler, K. Al-Sahlani, P. Linul, E. Linul, Mechanical properties of A356 and ZA27 metallic syntactic foams at cryogenic temperature, J. Alloys Compd. 813 (2020), 152181.
[19] N. Movahedi, M. Taherishargh, I. Belova, G. Murch, T. Fiedler, Mechanical and microstructural characterization of an AZ91–activated carbon syntactic foam, Materials 12 (2019) 3.
[20] N. Movahedi, G.E. Murch, I.V. Belova, T. Fiedler, Functionally graded metal syntactic foam: fabrication and mechanical properties, Mater. Des. 168 (2019), 107652.
[21] M.A. Kader, M.A. Islam, M. Saadatfar, P.J. Hazell, A.D. Brown, S. Ahmed, J.P. Escobedo, Macro and micro collapse mechanisms of closed-cell aluminium foams during quasi-static compression, Mater. Des. 118 (2017) 11–21.
[22] P.J. Tan, S.R. Reid, J.J. Harrigan, Z. Zou, S. Li, Dynamic compressive strength properties of aluminium foams. Part I—experimental data and observations, Journal of the Mechanics and Physics of Solids 53 (2005) 2174–2205.
[23] Y. Sun, Q.M. Li, T. Lowe, S.A. McDonald, P.J. Withers, Investigation of strain-rate effect on the compressive behaviour of closed-cell aluminium foam by 3D image-based modelling, Mater. Des. 89 (2016) 215–224.
[24] A. Bouterf, J. Adrien, E. Maire, X. Brajer, F. Hild, S. Roux, Identification of the crushing behavior of brittle foam: from indentation to oedometric tests, Journal of the Mechanics and Physics of Solids 98 (2017) 181–200.
[25] S. Ramachandra, P. Sudheer Kumar, U. Ramamurty, Impact energy absorption in an Al foam at low velocities, Scr. Mater. 49 (2003) 741–745.
[26] O. Olurin, N.A. Fleck, M.F. Ashby, Indentation resistance of an aluminium foam, Scr. Mater. 43 (2000) 983–989.
[27] H. Zhao, I. Elnasri, Y. Girard, Perforation of aluminium foam core sandwich panels under impact loading—an experimental study, International Journal of Impact Engineering 34 (2007) 1246–1257.
[28] I. Elnasri, H. Zhao, Impact perforation of sandwich panels with aluminum foam core: a numerical and analytical study, International Journal of Impact Engineering 96 (2016) 50–60.
[29] C. Liu, Y.X. Zhang, L. Ye, High velocity impact responses of sandwich panels with metal fibre laminate skins and aluminium foam core, International Journal of Impact Engineering 100 (2017) 139–153.
[30] E. Flores-Johnson, Q. Li, Low velocity impact on polymeric foams, J. Cell. Plast. 47 (2011) 45–63.
[31] W. Hou, F. Zhu, G. Lu, D.-N. Fang, Ballistic impact experiments of metallic sandwich panels with aluminium foam core, International Journal of Impact Engineering 37 (2010) 1045–1055.
[32] A. Xu, T. Vodenitcharova, K. Kabir, E.A. Flores-Johnson, M. Hoffman, Finite element analysis of indentation of aluminium foam and sandwich panels with aluminium foam core, Mater. Sci. Eng. A 599 (2014) 125–133.
[33] M.A. Islam, P.J. Hazell, J.P. Escobedo, M. Saadatfar, In-situ quasistatic compression and microstructural characterization of aluminium foams of different cell topology, in: XII International Conference on Applied Mechanics and Mechanical Engineering (ICAMME 2014), 2014 11–12.
[34] M.A. Islam, J.P. Escobedo, P.J. Hazell, G.J. Appleby-Thomas, M.Z. Quadir, Characterization of closed-cell aluminium foams subjected to compressive loading, TMS Annual Meeting 2015, pp. 167–174.
[35] M.A. Islam, A.D. Brown, P.J. Hazell, M.A. Kader, J.P. Escobedo, M. Saadatfar, S. Xu, D. Ruan, M. Turner, Mechanical response and dynamic deformation mechanisms of closed-cell aluminium alloy foams under dynamic loading, International Journal of Impact Engineering 114 (2018) 111–122.
[36] M.A. Islam, Dynamic Deformation Mechanics of Closed-cell Metallic Foams, PhD Dissertation 2018.
[37] Y. Sun, Q.M. Li, Dynamic compressive behaviour of cellular materials: a review of phenomenon, mechanism and modelling, International Journal of Impact Engineering 112 (2018) 74–115.
[38] A. Paul, U. Ramamurty, Strain rate sensitivity of a closed-cell aluminum foam, Mater. Sci. Eng. A 281 (2000) 1–7.
[39] D. Ruan, G. Lu, F.L. Chen, E. Siores, Compressive behaviour of aluminium foams at low and medium strain rates, Compos. Struct. 57 (2002) 331–336.
[40] U. Ramamurty, M. Kumaran, Mechanical property extraction through conical indentation of a closed-cell aluminum foam, Acta Mater. 52 (2004) 181–189.
[41] M. Kader, P. Hazell, A. Brown, M. Tahtali, S. Ahmed, J. Escobedo, M. Saadatfar, Novel design of closed-cell foam structures for property enhancement, Additive Manufacturing 31 (2019) 100976, https://doi.org/10.1016/j.addma.2019.100976.
[42] H.-W. Song, Q.-J. He, J.-J. Xie, A. Tobota, Fracture mechanisms and size effects of brittle metallic foams: in situ compression tests inside SEM, Compos. Sci. Technol. 68 (2008) 2441–2450.